IRANIAN JOURNAL OF CATALYSIS

Preparation, Characterization and Application of a Novel Organic-Inorganic Hybrid Magnetic Nanomaterial as a Highly Efficient Catalyst for the Synthesis of Bis-Coumarins

Marziyeh Barzegar*, Abdolkarim Zare*, Aysoda Ghobadpoor, Manije Dianat

Department of Chemistry, Payame Noor University, PO Box 19395-3697, Tehran, Iran.

ABSTRACT

A novel organic-inorganic hybrid magnetic nanomaterial, namely nano-[Fe_3O_4@SiO_2@R-NMe_2][$FeCl_4$] (nano-[FSRN][$FeCl_4$]) was prepared, and characterized by EDX, elemental mapping, FE-SEM, FT-IR, XRD, VSM, TG and DTG analyses. Then, it was applied as a highly efficient and magnetically recyclable catalyst for the solvent-free synthesis of bis-coumarins from 4-hydroxycoumarin (2 eq.) and arylaldehydes (1 eq.). NMe_2 is a basic group, and $FeCl_4^-$ is a Lewis acid; thus, nano-[FSRN][$FeCl_4$] can act as a dual-functional catalyst; based on this and the literature, a plausible mechanism was proposed for the reaction.

Keywords: Organic-inorganic hybrid magnetic nanomaterial, Nano-[Fe_3O_4@SiO_2@R-NMe_2][$FeCl_4$] (nano-[FSRN][$FeCl_4$]), Dual-functional catalyst, Bis-coumarin, Solvent-free.

1. Introduction

Organic-inorganic hybrid materials are composed of organic and inorganic components which interact together by van der Waals forces, hydrogen bonding, electrostatic interactions, covalent or ionic bonds [1]. Their properties depend on the organic and inorganic components characteristics, nature of the interfaces and ratio of each component [2]. The advantages of the hybrid materials include proper thermal and chemical durability, environmentally friendly nature, a wide range of uses, facile separation from the process reactor and efficacy. They have numerous uses in pharmaceutical and industrial fields. For instance, they have been utilized as highly hydrophobic coatings [3], drug carrier [4], semiconductor [5], nonlinear optical switch [6], and catalysts for organic transformations [7-13]. Applications of them in memories [14], transistors [14], artificial synapses [14], fuel cells [15], and sensors [16] have also been reported.

Magnetic nanomaterials have a wide range of uses in pharmacology and industry; their advantages have been mentioned in the literature [17-30]. In the field of organic chemistry, they have been especially applied as effective catalysts to promote reactions [23-30].

"Solvent-free conditions" has often superiority over solution conditions in organic synthesis; the superiority has been well explained in the literature [31-34].

Coumarin is a vital moiety in the structure of different biological and industrial compounds [35-49]. Coumarin-bearing compounds have shown antinociceptive [35], anticancer [35], antibacterial [35], anti-HIV [36], anti-Alzheimer [37], antifungal [38], antidiabetic [39] and anti-inflammatory [40] properties. Bis-coumarins have been used as anticoagulant [41], urease inhibitory [42], cytotoxicity [43], enzyme inhibitory [43], antioxidant [44], antimicrobial [44], anti-parasite [45], antibacterial [46] and anti-inflammatory [46] agents; they have been also utilized for the detection of hydrazine and palladium in natural waters [47,48], and sensing phosdrin pesticide [49]. Bis-coumarins can be synthesized through the reaction of 4-hydroxycoumarin (2 eq.) and arylaldehydes (1 eq.) in the presence of a catalyst [50-59].

*Corresponding author:
E-mail address: *barzegar.marziyeh@yahoo.com* (**M. Barzegar**);abdolkarimzare@pnu.ac.ir;abdolkarimzare@yahoo.com (**A. Zare**)

In this research, we have prepared a novel organic-inorganic hybrid magnetic nanomaterial, namely nano-[Fe_3O_4@SiO_2@R-NMe_2][$FeCl_4$] (nano-[FSRN][$FeCl_4$]), and characterized it by EDX (energy-dispersive X-ray spectroscopy), elemental mapping, FE-SEM (field emission scanning electron microscopy), FT-IR (Fourier-transform infrared spectroscopy), XRD (X-ray diffraction), VSM (vibrating-sample magnetometry), TG (thermal gravimetric) and DTG (differential thermal gravimetric) analyses. Then, we have used it as a highly efficient, magnetically recyclable and dual-functional catalyst for the solvent-free synthesis of bis-coumarins through the reaction of 4-hydroxycoumarin and arylaldehydes.

2.Experimental

2.1. Chemicals and instruments

Information on the used chemicals and instruments have been given in supplementary information.

2.2. Procedure for the preparation of nano-[Fe₃O₄@SiO₂@R-NMe₂][FeCl₄] (nano-[FSRN][FeCl₄])

A reported method was used for the preparation of nano-Fe_3O_4 [60,61]. A mixture of nano-Fe_3O_4 (0.75 g), Si(OEt)$_4$ (2.25 mL), H_2O (15 mL), EtOH (60 mL) and ammonia (2.4 mL) was stirred under reflux conditions for 12 h to provide compound I. Then, (3-chloropropyl)trimethoxysilane (1.38 mL, 7.5 mmol) and dry toluene (60 mL) were added to I, and stirred under reflux conditions and flowing nitrogen gas for 12 h to afford II [61,62]. A mixture of II and N,N,N′,N′-tetramethylethane-1,2-diamine (1.12 mL, 7.5 mmol) in dry toluene (45 mL) was stirred and refluxed for 12 h to give compound III [28]. Finally, $FeCl_3$ (1.22 g, 7.5 mmol) was added to III in MeCN (20 mL) at room temperature, and the resulting mixture was stirred for 24 h under reflux conditions to afford nano-[FSRN][FeCl4]; this step was performed based on the literature for the similar cases [63,64].

Note: Before each step, the reaction mixture was dispersed by ultrasound irradiation. Moreover, the precursors for the catalyst synthesis (Fe_3O_4 and compounds I-III) were magnetically separated from the reaction mixture (or by centrifuging and decanting), washed by the solvent used in that step, and dried (**Scheme 1**).

2.3. General procedure for the synthesis of bis-coumarins

A mixture of 4-hydroxycoumarin (0.325 g, 2 mmol), aldehyde (1.1 mmol) and nano-[FSRN][$FeCl_4$] (0.08 g) was strongly stirred by a rod at 100 °C. When TLC showed consuming the reactants, the reaction mixture was cooled to room temperature, EtOAc (30 mL) was added, and stirred for 2 min in reflux conditions; the insolvable catalyst was separated magnetically (washed by EtOAc, and dried). EtOAc of the remaining solution was distilled, and the obtained precipitate was recrystallized from EtOH (95%) to afford the pure product.

3. Results and Discussion

3.1. Characterization of the catalyst

Nano-[Fe_3O_4@SiO_2@R-NMe_2][$FeCl_4$] (nano-[FSRN][$FeCl_4$]) was prepared according to **Scheme 1** (the experimental section), and characterized by EDX, elemental mapping, FE-SEM, FT-IR, XRD, VSM, TG and DTG analyses.

The EDX spectrum of nano-[FSRN][$FeCl_4$] is displayed in **Fig. 1**. The spectrum approved presence of C, N, O, Fe, Si and Cl elements in the nanomaterial structure (as expected). Presence of these elements in the structure of nano-[FSRN][$FeCl_4$] was also verified by elemental mapping analysis, as illustrated in **Fig. 2**. Furthermore, the elemental mapping images showed well distribution of C, N, O, Fe, Si and Cl in the catalyst surface.

To determine size and morphology of the catalyst particles, FE-SEM was utilized; the obtained images are shown in **Fig. 3**. As it can be seen in **Fig. 3**, sizes of the particles are less than 100 nm, i.e. the catalyst is a nanomaterial. Additionally, the particles of nano-[FSRN][$FeCl_4$] have different crystalline shapes.

In the FT-IR spectrum of nano-[FSRN][$FeCl_4$] (**Fig. 4**), the peaks observed at 470 and 585 cm^{-1} are related to Si–O (rocking) and Fe–O bonds, respectively. The peaks correspond to symmetric and asymmetric stretching vibrations of Si–O–Si were seen at 803 and 1099 cm^{-1}, respectively. C–H bonds (stretching vibration) of the alkyl chain anchored with Fe_3O_4@SiO_2 surface gave a peak at 2930 cm^{-1}. The broad peak observed at ~2500-3720 cm^{-1} corresponded to OH groups on the silica surface (stretching) [30].

The XRD patterns of nano-[FSRN][$FeCl_4$] and nano-Fe_3O_4 (**Fig. 5** and **6**) showed some diffraction lines of crystalline nature, which are reported in the first column of **Table 1**; the peaks observed at 2θ = 30.2619, 35.7792, 43.4652, 53.8666, 57.3336 and 62.8412° in the XRD pattern of nano-[Fe_3O_4@SiO_2@R-NMe_2][$FeCl_4$] confirmed presence of a cubic spinel structure of Fe_3O_4 in its structure (compare **Fig. 5** and **6**); the broad peak at 2θ ≈ 19.4-29.0° is related to the amorphous structure of the SiO_2 layer [64]. The peak width (full width at half maximum, FWHM), interplanar distance, relative

intensity of the peaks and crystalline sizes of the particles were also determined, and are shown in **Table 1**. For instance, FWHM, interplanar distance and crystalline size for the highest diffraction line (2θ = 35.7792°) are 0.2952°, 0.2510 nm and 28.30 nm, respectively. The interplanar distance (d) for the diffraction line was obtained by the Bragg equation {d = λ/(2sin θ), in which λ is Cu radiation wavelength (0.154178 nm)}; the crystalline size (D) for the

diffraction line was obtained by Debye–Scherrer equation {D = Kλ/(βcos θ), where K is the shape factor (0.9), λ is Cu radiation wavelength (0.154178 nm), and β is the FWHM of the diffraction peak in radian}. The crystallite sizes of nano-[FSRN][FeCl$_4$], determined by Debye–Scherrer equation, were in the range of 11.33-47.34 nm, and are in good compliance with the results obtained from FE-SEM (**Fig. 3**).
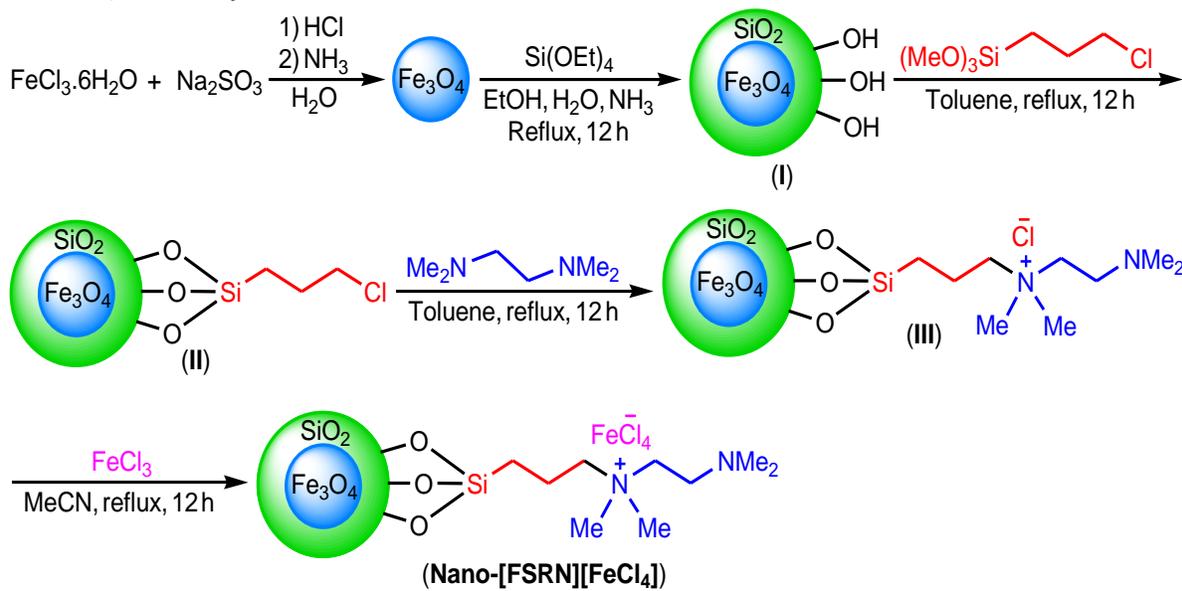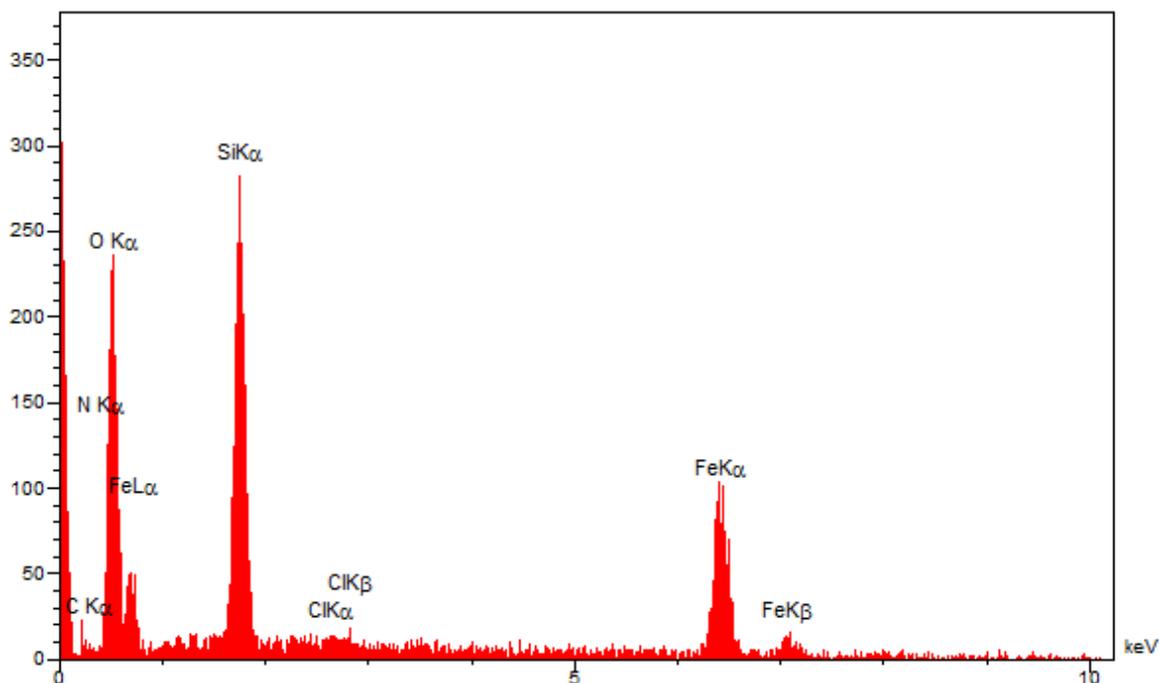

Scheme 1. The preparation of nano-[FSRN][FeCl4].

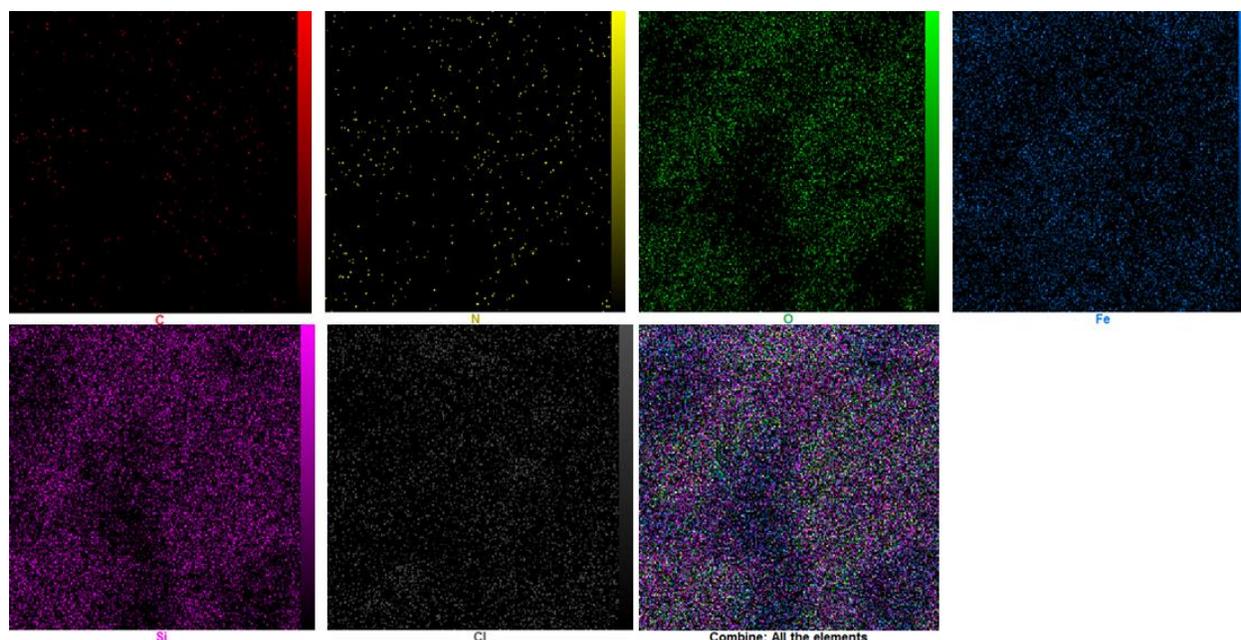**Fig. 1.** The EDX spectrum of nano-[FSRN][FeCl$_4$].

Fig. 2. The elemental mapping images of nano-[Fe$_3$O$_4$@SiO$_2$@R-NMe$_2$][FeCl$_4$].
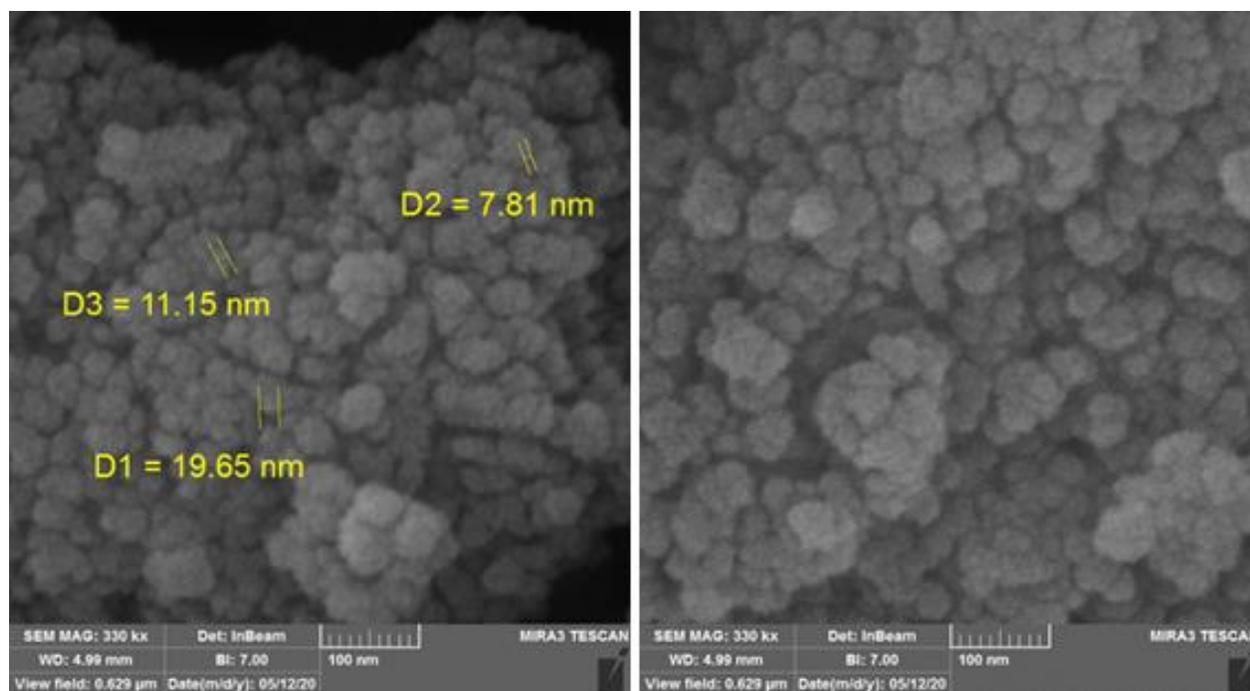

Fig. 3. The FE-SEM images of the catalyst.

To study magnetic property of nano-[Fe$_3$O$_4$@SiO$_2$@R-NMe$_2$][FeCl$_4$], a vibrating sample magnetometer was applied (the study was achieved at room temperature); the obtained diagram is represented in **Fig. 7**; saturation magnetization of nano-[FSRN][FeCl$_4$] was ~39.7 emu.g^{-1}. It is worth noting that saturation magnetization of compound **III** (**Scheme 1**), as the precursor for the synthesis of nano-[FSRN][FeCl$_4$], was ~37 emu.g^{-1} (**Fig. 8**); the increase of saturation magnetization after performing the reaction of **III** with FeCl$_3$ can be related

to formation of FeCl$_4^-$ [65]. Moreover, saturation magnetization of the used nano-Fe$_3$O$_4$ for the synthesis of nano-[FSRN][FeCl$_4$] was ~56.7 emu.g^{-1} (**Fig. 9**). The diminution of saturation magnetization in nano-[FSRN][FeCl$_4$] compared with nano-Fe$_3$O$_4$ can be attributed to coating silica on the nano-Fe$_3$O$_4$, and grafting the organic moieties with the Fe$_3$O$_4$@SiO$_2$ surface. Nevertheless, nano-[FSRN][FeCl$_4$] was properly magnetized, and could magnetically separate from the reaction mixture.
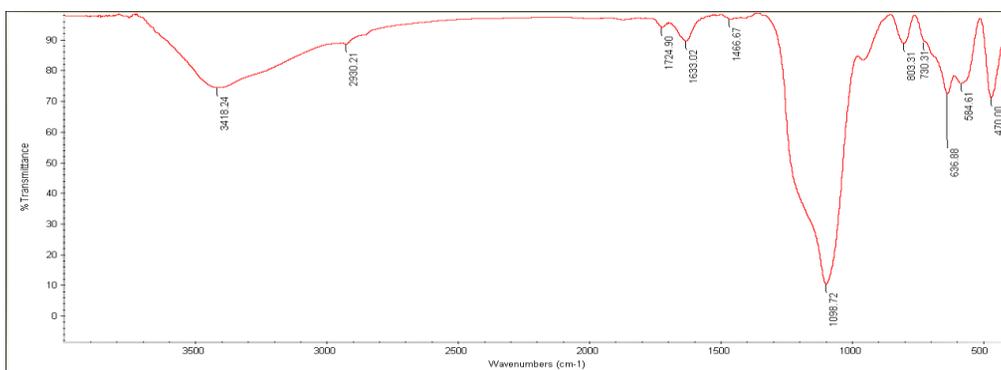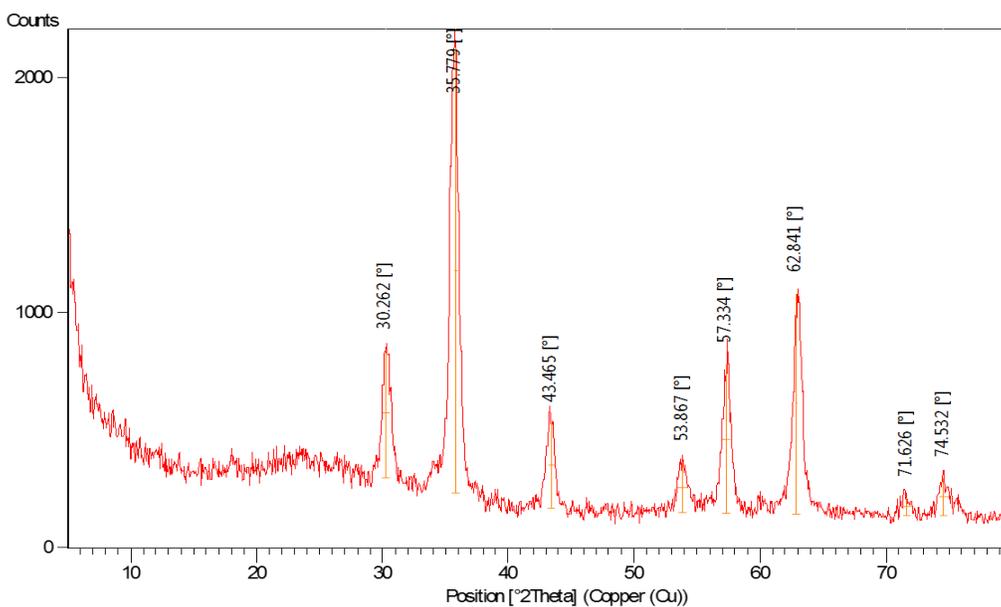
Fig. 4. The FT-IR spectrum of the nanomaterial.

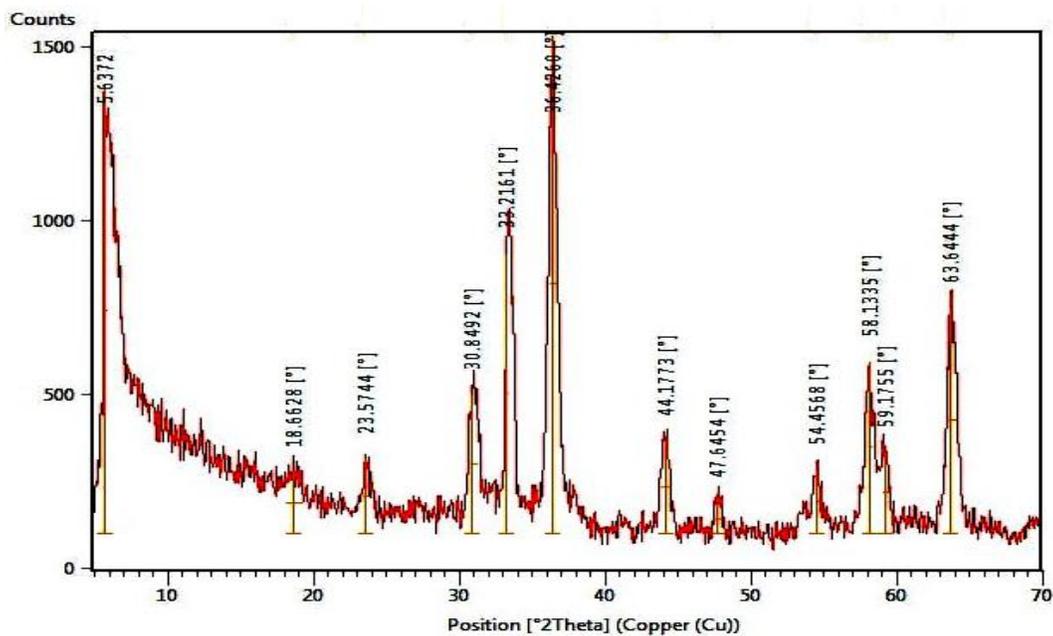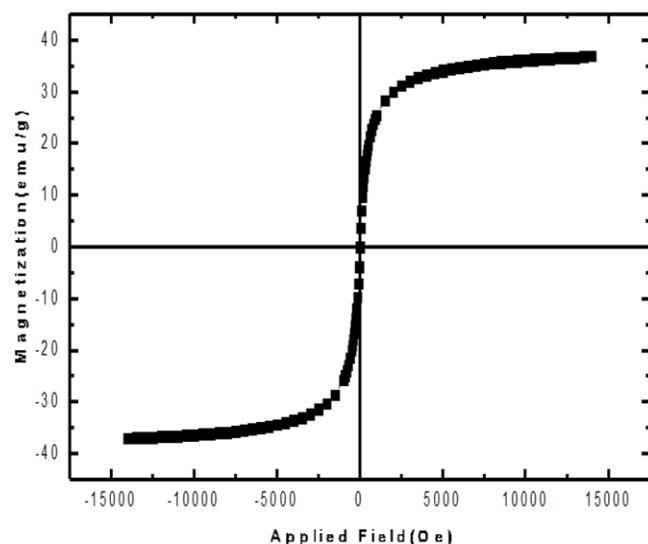**Fig. 5.** The XRD pattern of nano-[FSRN][FeCl₄].
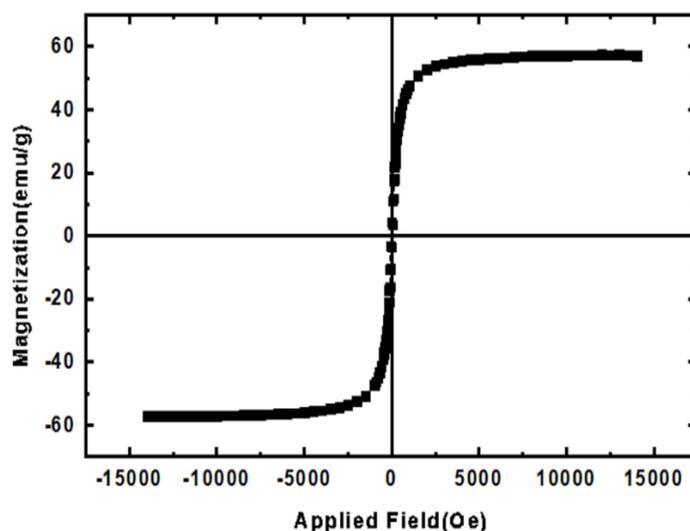

Fig. 6. The XRD pattern of nano- Fe_3O_4 used for the catalyst synthesis.

Table 1. The XRD data of nano-[FSRN][FeCl$_4$].

2θ (°)	Peak width, FWHM (°)	Interplanar Distance (nm)	Rel. int. (%)	Crystalline size (nm)
30.2619	0.5904	0.2953	28.82	13.95
35.7792	0.2952	0.2510	100.00	28.30
43.4652	0.5904	0.2082	19.28	14.50
53.8666	0.7872	0.1702	11.23	11.33
57.3336	0.6888	0.1607	33.32	13.16
62.8412	0.1968	0.1479	49.63	47.34
71.6256	0.7872	0.1318	4.03	12.45
74.5325	0.7872	0.1273	8.51	12.69
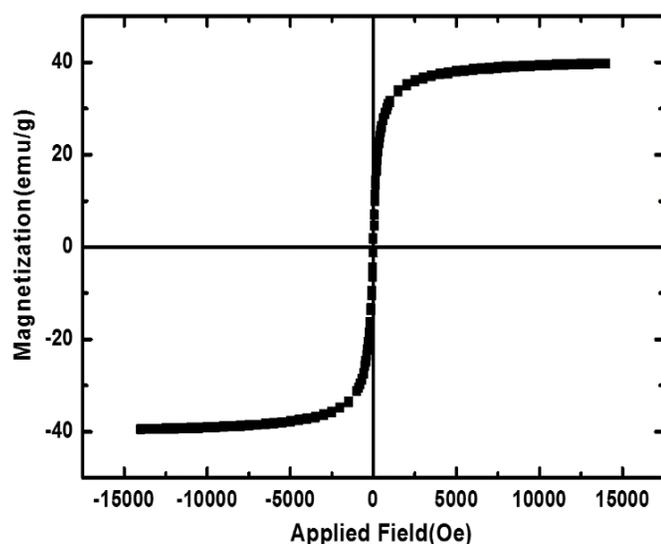
Fig. 7. The VSM diagram of nano-[FSRN][FeCl$_4$].

Fig. 9. The VSM diagram of nano-Fe$_3$O$_4$.

Fig. 8. The VSM diagram of compound **III**.

TG and DTG analyses were utilized to study thermal stability of nano-[FSRN][FeCl$_4$] (**Fig. 10**). Weight losses of the catalyst occurred in three steps: (i) below 125 ℃, which can be related to evaporation of the absorbed solvents on the Fe$_3$O$_4$@SiO$_2$ surface, (ii) about 125-430 ℃ (with T$_{max}$ at 262 ℃ in DTG diagram), which may be due to loss of NHMe$_2$ and the other organic groups in the catalyst structure, conversion of FeCl$_4^-$ to FeCl$_3$, and oxidation of FeCl$_4^-$, and (iii) about 430-600 ℃ (with T$_{max}$ at 443 ℃ in DTG diagram) which can be attributed to the condensation of the silanol groups [8].

3.2. Application of nano-[FSRN][FeCl$_4$] as catalyst for the synthesis of bis-coumarins

Optimization of the reaction conditions was achieved by studying effect of the catalyst dosage and temperature on a model reaction {the condensation of 4-

hydroxycoumarin (2 mmol) with 4-chlorobenzaldehyde (1.1 mmol)} (**Scheme 2**)}. The results are summerized in Table 2; when 0.065 g of nano-[FSRN][FeCl$_4$] was used at 90-110 ℃, the desired bis-coumarin was produced in moderate to good yields (**Table 2**, entries 1-3). Testing the reaction using 0.080 g of the catalyst at 90 ℃ failed to give satisfactory results (**Table 2**, entry 4). The best results were reported when the reaction was performed in the presence of 0.080 g of nano-[FSRN][FeCl$_4$] at 100 ℃ (**Table 2**, entry 5). The reaction temperature was raised up to 110 ℃ and the catalyst dosage up to 0.100 g, but no improvement in the results was observed (**Table 2**, entries 6 and 7).

Scope and effectiveness of nano-[FSRN][FeCl$_4$] for the production of bis-coumarins were evaluated by reacting 4-hydroxycoumarin with miscellaneous aromatic aldehydes, including benzaldehyde and arylaldehydes possessing electron-attracting, halogen and electron-donating substituents on *ortho*, *meta* or *para* positions;

the obtained results are represented in **Table 3**. The very good results (i.e. the synthesis of all bis-coumarins in high yields and relatively short times) approved wide scope and high effectiveness of the catalyst.

Nano-[Fe$_3$O$_4$@SiO$_2$@R-NMe$_2$][FeCl$_4$] can act as a dual-functional (acidic-basic) catalyst; FeCl$_4^-$ is a Lewis acid, and NMe$_2$ group is a base. Based on this issue and the literature [50,51], a plausible mechanism was designed for the reaction (**Scheme 3**); the catalyst roles are clearly illustrated in the mechanism. The acidic moiety can activate the electrophiles to accept nucleophiles in steps 1 and 3; FeCl$_4^-$ can also facilitate removal of H$_2$O (step 2) and tautomerization (step 4). The basic moiety can activate the nucleophiles to carry out steps 1 and 3; NMe$_2$ can also help removing H$_2$O (step 2) and tautomerization (step 4).
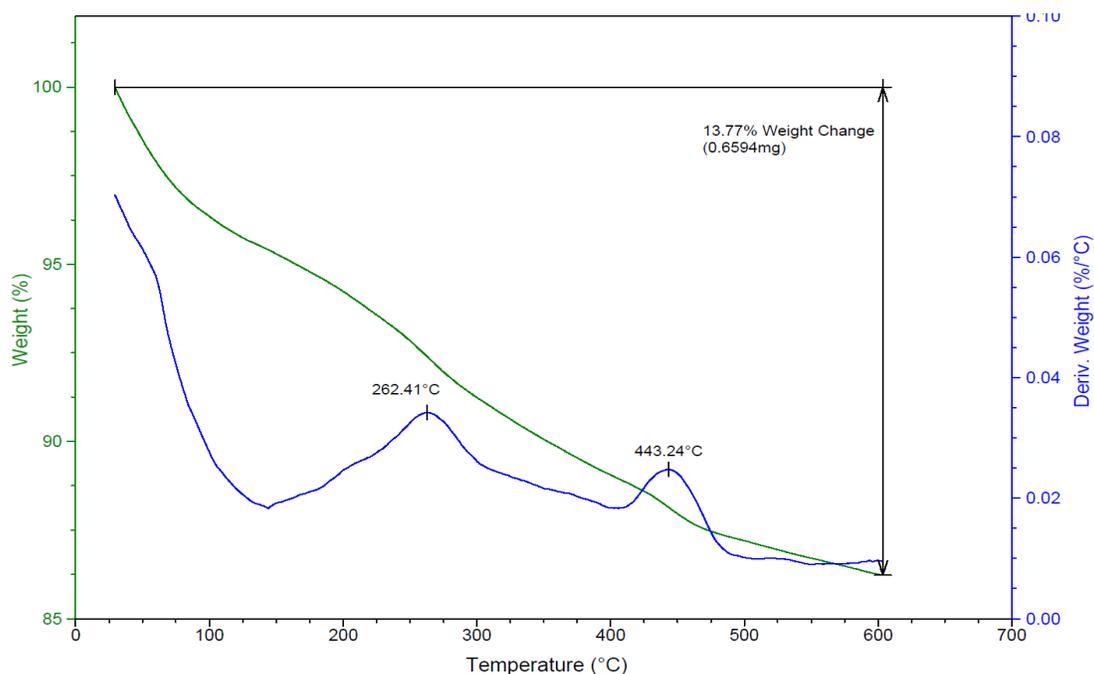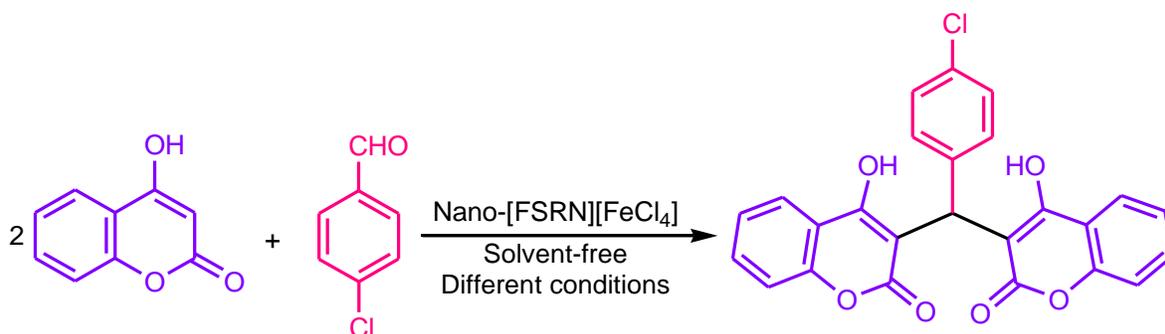

Fig. 10. The TG and DTG diagrams of nano-[FSRN][FeCl$_4$].

Scheme 2. The reaction of 2-hydroxynaphthoquinone with 4-chlorobenzaldehyde.

Table 2. Effect of the catalyst dosage and temperature on the model reaction.

Entry	Nano-[FSRN][FeCl$_4$] (g)	Temp. (ºC)	Time (min)	Yield (%)
1	0.065	90	30	74
2	0.065	100	30	82
3	0.065	110	30	88
4	0.080	90	30	92
5	0.080	100	15	95[a]
6	0.080	110	15	95[a]
7	0.100	100	15	95[a]

[a]The reaction was almost completed.

Table 3. The synthesis of various derivatives of bis-coumarins catalyzed by nano-[FSRN][FeCl$_4$].
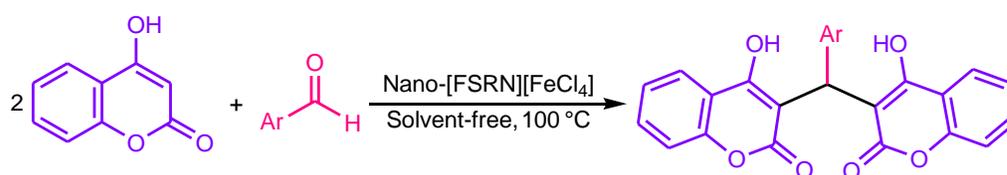
| Product No.	Ar	Time (min)	Yield [a] (%)	M.p. (ºC) [lit.]
1	C$_6$H$_5$	15	93	228-230 (229-231) [50]
2	4-CH$_3$C$_6$H$_4$	30	96	265-267 (267-270) [57]
3	2,5-(CH$_3$O)$_2$C$_6$H$_3$	30	85	191-193 (188-190) [58]
4	3,4-(CH$_3$O)$_2$C$_6$H$_3$	25	91	262-264 (264-266) [54]
5	4-CH$_3$OC$_6$H$_4$	20	93	242-244 (243-245) [51]
6	4-(Me$_2$N)C$_6$H$_4$	20	87	225-227 (223-225) [54]
7	3-O$_2$NC$_6$H$_4$	25	96	234-236 (236-238) [51]
8	4-Cl-3-O$_2$NC$_6$H$_3$	15	94	259-261 (250-252) [56]
9	2-ClC$_6$H$_4$	30	88	215-217 (218-220) [58]
10	4-ClC$_6$H$_4$	15	95	253-255 (254-256) [50]
11	4-BrC$_6$H$_4$	25	93	263-265 (262-264) [57]
12	4-FC$_6$H$_4$	20	94	208-210 (210-212) [58]

[a]Isolated yield.

In **Table 4**, nano-[FSRN][FeCl$_4$] was compared with some reported catalysts for the production of bis-coumarins; for this purpose, products **1** and **10** were chosen. Our catalyst is superior than the catalysts reported in Table 4 in term of two or more of following factors: the reaction time, yield, medium (solvent-free versus utilization of organic solvents) and temperature.

Recyclability of nano-[FSRN][FeCl$_4$] was investigated on the model reaction (**Scheme 2**). It was recycled according to the mentioned procedure in the

experimental section, and reused. According to the results given in **Fig. 11**, nano-[FSRN][FeCl₄] was reused for three times without remarkable reduction of the yield and increase of the reaction time (runs 1-4);

nevertheless, low decreasing in the yield was observed in fourth recycling and reusing (**Fig. 11**, run 5).
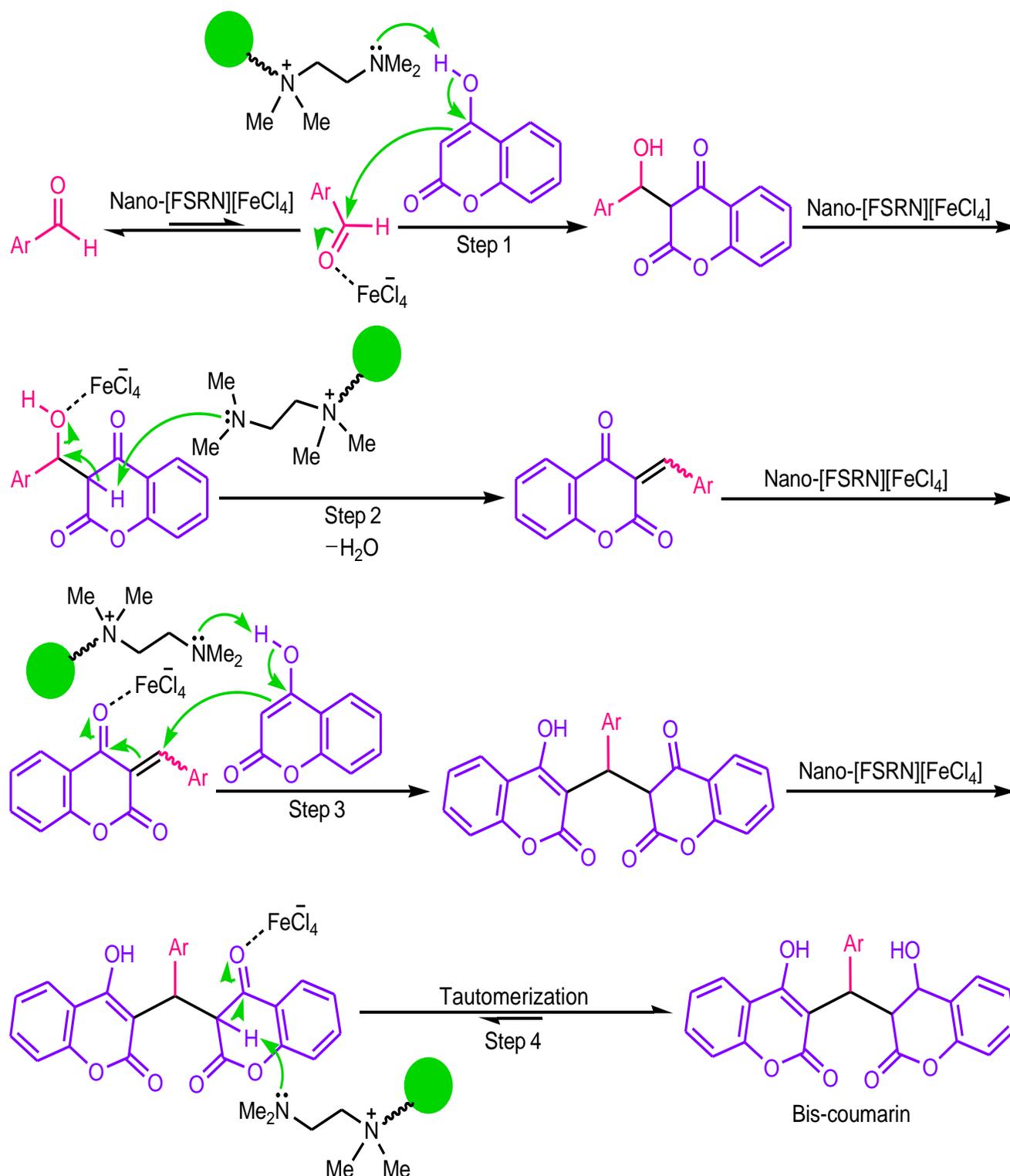
Scheme 3. The reaction mechanism.

Table 4. Comparing the reaction conditions and the results of nano-[FSRN][FeCl$_4$] with those of some reported catalysts for the production of bis-coumarins

Catalyst	Conditions	Time (min) of product 1/10	Yield (%) of product 1/10	Ref.
Nano-[FSRN][FeCl$_4$]	Solvent-free, 100 ℃	15/15	93/95	-
Co$_3$O$_4$/NiO@GQDs@SO$_3$H	EtOH, ultrasonic irradiation	10/10	90/92	[50]
[P$_4$VPy-BuSO$_3$H]HSO$_4$[a]	Toluene, 90 ℃	48/48	93/94	[51]
Fe$_3$O$_4$@SiO$_2$@Im-bisethylFc[HC$_2$O$_4$][b]	EtOH, reflux	180-315	84-93	[52]
[P$_4$VPy-BuSO$_3$H]Cl-X(AlCl$_3$)	Toluene, 90 ℃	36/36	95/93	[53]
Catalyst-free	Ethylene glycol, 90 ℃	90/90	84/94	[54]
Porcine pancreas lipase	EtOH, 45 ℃	360/240	85/84	[55]
CuFe$_2$O$_4$@SiO$_2$@AAPTMS @Ni(II)	H$_2$O, reflux	12/24	96/89	[56]
CuFe$_2$O$_4$@SiO$_2$@AAPTMS @Cu(II)	H$_2$O, reflux	18/25	95/85	[56]
Fe$_3$O$_4$@SiO$_2$@VB$_1$-Ni^{2+}	Solvent-free, 110 ℃	30/35	95/85	[57]
APVPB	Solvent-free, 70 ℃	17/15	88/92	[58]
Sodium dodecyl sulfate	H$_2$O, 60 ℃	150/150	90/93	[59]

[a]Poly(4-vinylpyridine-1-sulfonic acid-butyl-4-vinylpyridinium)hydrogen sulfate. [b]In this work, compounds **1** and **10** have not been synthesized; therefore, we reported the range of times and yields. [c]Acetic acid functionalized poly(4-vinylpyridinum) bromide
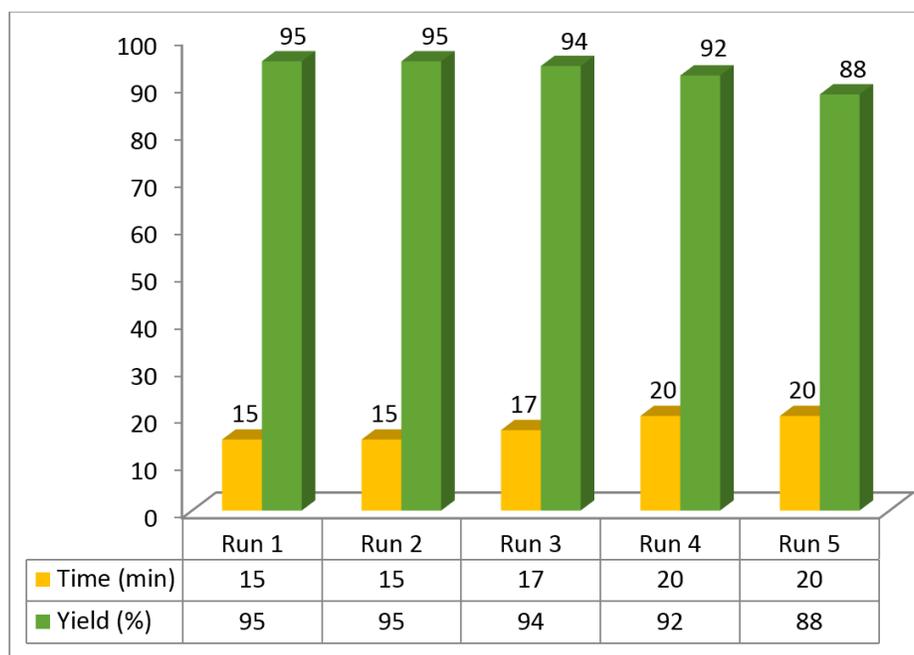
Fig. 11. The results of reusability of nano-[FSRN][FeCl$_4$].

4. Conclusions

Briefly, we have introduced a novel organic-inorganic hybrid nanomaterial (nano-[FSRN][FeCl$_4$]) as a catalyst for organic transformations. In this work, it has successfully catalyzed the production of bis-coumarins, with several advantages including relatively short reaction times, high yields, wide scope, efficacy, performing the synthesis in solvent-free conditions, dual-functionality of the catalyst, simple workup and purification of the products, and being in good agreement with green chemistry principles.

Acknowledgements

References

[1] S. Montes, H. Maleki, Colloidal Metal Oxide Nanoparticles: Synthesis, Characterization and Applications, S. Thomas, A. T. Sunny, P. Velayudhan (Ed.), Elsevier (2020), https://doi.org/10.1016/C2016-0-03725-7.

[2] C. Sanchez, B. Julián, P. Belleville, M. Popall, J. Mater. Chem. 15 (2005) 3559-3592.

[3] C.-H. Yang, Y.-W. Pan, J.-J. Guo, T.-H. Young, W.-Y. Chiu, K.-H. Hsieh, J. Polym. Res. 23 (2016) 29.

[4] P. Huang, Y. Chen, H. Lin, L. Yu, L. Zhang, L. Wang, Y. Zhu, J. Shi, Biomaterials 125 (2017) 23-37.

[5] B. Zhang, Y. Zhang, Z. Wang, D. Yang, Z. Gao, D. Wang, Y. Guo, D. Zhu, T. Mori, Dalton Trans. 45 (2016) 16561-16565.

[6] X. Liu, C. Ji, Z. Wu, L. Li, S. Han, Y. Wang, Z. Sun, J. Luo, Chem. Eur. J. 25 (2019) 2610-2615.

[7] F. Jalili, M. Zarei, M. A. Zolfigol, S. Rostamnia, A. R. Moosavi-Zare, Micropor. Mesopor. Mater. 294 (2020) 109865.

[8] A. Zare, F. Monfared, S. S. Sajadikhah, Appl. Organomet. Chem. 34 (2020) e6046.

[9] P. Moradi, M. Hajjami, New J. Chem. 45 (2021) 2981-2994.

[10] A. Zare, R. Khanivar, N. Irannejad-Gheshlaghchaei, M. H. Beyzavi, ChemistrySelect 4 (2019) 3953-3960.

[11] M. Shekouhy, R. Kordnezhadian, A. Khalafi-Nezhad, J. Iran. Chem. Soc. 15 (2018) 2357-2368.

[12] A. Shamaei, B. Mahmoudi, M. Kazemnejadi, M. A. Nasseri, Appl. Organomet. Chem. 34 (2020) e5997.

[13] A. Zare, M. Dianat, M. M. Eskandari, New J. Chem. 44 (2020) 4736-4743.

[14] J. Choi, J. S. Han, K. Hong, S. Y. Kim, H. W. Jang, Adv. Mater. 30 (2018) 1704002.

[15] T. Feng, B. Lin, S. Zhang, N. Yuan, F. Chu, M. A. Hickner, C. Wang, L. Zhu, J. Ding, J. Membr. Sci. 508 (2016) 7-14.

[16] G. Mohammadi Ziarani, V. Fathi Vavsari, A. Badiei, J. Afshani, P. Gholamzadeh, S. Balalaie, F. Faridbod, M. R. Ganjali, J. Iran. Chem. Soc. 15 (2018) 211-221.

[17] V. Mohammadi, M. Tabatabaee, A. Fadaei, S. A. Mirhoseini, Iran. J. Catal. 10 (2020 209-218.

[18] Z. Karimi Ghezeli, M. Hekmati, H. Veisi, Appl. Organomet. Chem. 33 (2019) e4833.

[19] R. Doaga, T. McCormac, E. Dempsey, Microchim. Acta 187 (2020) 225.

[20] F. Gao, ChemistrySelect 4 (2019) 6805-6811.

[21] S. Azizi, H. Nosrati, H. Danafar, Appl. Organomet. Chem. 34 (2020) e5479.

[22] R. K. Gautam, I. Tiwari, Chemosphere 245 (2020) 125553.

[23] J. Safari, M. Tavakoli, M. A. Ghasemzadeh, Polyhedron 182 (2020) 114459.

[24] M. A. Ghasemzadeh, B. Mirhosseini-Eshkevari, M. Tavakoli, F. Zamani, Green Chem. 22 (2020) 7265-7300.

[25] S. Sajjadifar, I. Amini, M. Karimian, Iran. J. Catal. 11 (2021) in press.

[26] F. Gholami Orimi, B. Mirza, Z. Hossaini, Appl. Organomet. Chem. 35 (2021) e6193.

[27] E. Babaei, B. B. F. Mirjalili, Iran. J. Catal. 10 (2020) 219-226.

[28] A. Zare, N. Lotfifar, M. Dianat, J. Mol. Struct. 1211 (2020) 128030.

[29] Z. Kheilkordi, G. Mohammadi Ziarani, A. Badiei, H. Vojoudi, Iran. J. Catal. 10 (2020) 65-70.

[30] A. Zare, M. Barzegar, Res. Chem. Intermed. 46 (2020) 3727-3740.

[31] M. Himaja, D. Poppy, K. Asif, Int. J. Res. Ayurveda Pharm. 2 (2011) 1079-1086.

[32] Z. Abshirini, A. Kohzadian, Z. Paryav, A. Zare, Iran. J. Catal. 9 (2019) 251-257.

[33] F. Tamaddon, S. E. Tadayonfar, J. Mol. Liq. 280 (2019) 71-78.

[34] A. Zare, A. Kohzadian, Z. Abshirini, S. S. Sajadikhah, J. Phipps, M. Benamarad, M. H. Beyzavi, New J. Chem. 43 (2019) 2247-2257.

[35] J. H. Lee, H. B. Bang, S. Y. Han, J. G. Jun, Tetrahedron Lett. 48 (2007) 2889-2892.

[36] H. Zhao, N. Neamati, H. Hong, H. A. Mazumder, S. Wang, S. Sunder, G. W. A. Milne, Y. Pommier, T. R. Burke, J. Med. Chem. 40 (1997) 242-249.

[37] P. Anand, B. Singh, N. Singh, Bioorg. Med. Chem. 20 (2012) 1175-1180.

[38] A. A. Al-Amiery, A. A. H. Kadhum, A. B. Mohamad, Molecules 17 (2012) 5713-5723.

[39] H. Li, Y. Yao, L. Li, J. Pharm. Pharmacol. 69 (2017) 1253-1264.

[40] L. Z. Chen, W. W. Sun, L. Bo, J. Q. Wang, C. Xiu, W. J. Tang, J. B. Shi, H. P. Zhou, X. H. Liu, Eur. J. Med. Chem. 138 (2017) 170-181.

[41] I. Manolov, C. Maichle-Moessmer, I. Nicolova, N. Danchev, Arch. Pharm. 339 (2006) 319-326.

[42] K. M. Khan, S. Iqbal, M. A. Lodhi, G. M. Maharvi, Zia-Ullah, M. I. Choudhary, Atta-ur-Rahman, S. Perveen, Bioorg. Med. Chem. 12 (2004) 1963-1968.

[43] M. Choudhary, N. Fatima, K. M. Khan, S. Jalil, S. Iqbal, Atta-ur-Rahman, Bioorg. Med. Chem. 14 (2006) 8066-8072.

[44] N. Hamdi, M. C. Puerta, P. Valerga, Eur. J. Med. Chem. 43 (2008) 2541-2548.

[45] Q.-C. Ren, C. Gao, Z. Xu, L.-S. Feng, M.-L. Liu, X. Wu, F. Zhao, Curr. Top. Med. Chem. 18 (2018) 101-113.

[46] B. M. Chougala, S. Samundeeswari, M. Holiyachi, N. S. Naik, L. A. Shastri, S. Dodamani, S. Jalalpure, S. R. Dixit, S. D. Joshi, V. A. Sunagar, Eur. J. Med. Chem. 143 (2018) 1744-1756.

[47] X. Jiang, M. Shangguan, Z. Lu, S. Yi, X. Zeng, Y. Zhang, L. Hou, Tetrahedron 76 (2020) 130921.

[48] C. Chen, L. Zhou, F. Liu, Z. Li, W. Liu, W. Liu, J. Hazard. Mater. 386 (2020) 121943.

[49] B. H. M. Hussein, G. M. Khairy, R. M. Kamel, Spectrochim. Acta A: Mol. Biomol. Spectrosc. 158 (2016) 34-42.

[50] H. Shahbazi-Alavi, A. K. Abbas, J. Safaei-Ghomi, Nanocomposites 6 (2020) 56-65.

[51] K. Parvanak Boroujeni, P. Ghasemi, Z. Rafienia, Monatsh. Chem. 145 (2014) 1023-1026.

[52] R. Teimuri-Mofrad, S. Tahmasebi, E. Payami, Appl. Organomet. Chem. 33 (2019) e4773.

[53] K. Parvanak Boroujeni, P. Ghasemi, Catal. Commun. 37 (2013) 50-54.

[54] S. S. Kauthale, S. U. Tekale, K. M. Jadhav, R. P. Pawar, Mol. Divers. 20 (2016) 763-770.

[55] H. Bavandi, Z. Habibi, M. Yousefi, Bioorg. Chem. 103 (2020) 104139.

[56] B. Zeynizadeh, M. Sadeghbari, N. Noroozi Pesyan, J. Iran. Chem. Soc. 17 (2020) 73-88.

[57] N. Azizi, F. Abbasi, M. Abdoli-Senejani, ChemistrySelect 3 (2018) 3797-3802.

[58] E. Noroozizadeh, A. R. Moosavi-Zare, M. A. Zolfigol, M. Zarei, R. Karamian, M. Asadbegy, S. Yari, S. H. Moazzami Farida, J. Iran. Chem. Soc. 15 (2018) 471-481.

[59] H. Mehrabi, H. Abusaidi, J. Iran. Chem. Soc. 7 (2010) 890-894.

[60] S. Qu, H. Yang, D. Ren, S. Kan, G. Zou, D. Liand, M. Li, J. Colloid Interf. Sci. 215 (1999) 190-192.

[61] M. A. Zolfigol, R. Ayazi-Nasrabadi, S. Baghery, Appl. Organomet. Chem. 30 (2016) 500-509.

[62] Y. H. Deng, C. C. Wang, J. H. Hu, W. L. Yang, S. K. Fu, Colloids Surf. A 262 (2005) 87-93.

[63] Y.-L. Hu, B.T. Wang, D. Fang, J. Iran. Chem. Soc. 14 (2017) 233-243.

[64] A. Alizadeh, M. Fakhari, M. M. Khodeai, G. Abdi, J. Amirian, RSC Adv. 7 (2017) 34972-34983.

[65] X. Pei, Y.H. Yan, L. Yan, P. Yang, J. Wang, R. Xu, M.B. Chan-Park, Carbon 48 (2010) 2501-2505.